



Bergische Universität Wuppertal

Fachbereich Mathematik und Naturwissenschaften

Lehrstuhl für Angewandte Mathematik  
und Numerische Mathematik

Lehrstuhl für Optimierung und Approximation

Preprint BUW-AMNA-OPAP 09/04

Matthias Ehrhardt, Jürgen Fuhrmann and Alexander Linke

**A model of an electrochemical flow cell  
with porous layer**

October 2009

<http://www.math.uni-wuppertal.de>

## A MODEL OF AN ELECTROCHEMICAL FLOW CELL WITH POROUS LAYER

MATTHIAS EHRHARDT

Lehrstuhl für Angewandte Mathematik und Numerische Analysis,  
Fachbereich Mathematik und Naturwissenschaften, Bergische Universität Wuppertal,  
Gaußstrasse 20, 42119 Wuppertal, Germany

JÜRGEN FUHRMANN

Weierstrass Institute for Applied Analysis and Stochastics,  
Mohrenstrasse 39, 10117 Berlin, Germany

ALEXANDER LINKE

Weierstrass Institute for Applied Analysis and Stochastics,  
Mohrenstrasse 39, 10117 Berlin, Germany

(Communicated by the associate editor name)

**ABSTRACT.** In this paper we discuss three different mathematical models for fluid–porous interfaces in a simple channel geometry that appears e.g. in thin-layer channel flow cells. Here the difficulties arise from the possibly different orders of the corresponding differential operators in the different domains. A finite volume discretization of this model allows to calculate the limiting current of the  $H_2$  oxidation in a porous electrode with platinum catalyst particles.

**1. Introduction.** Numerical simulation of coupled flows in plain and porous media is essential for many industrial and environmental problems. Here we shortly review coupling conditions between the pure liquid flow and the flow in a porous medium. We will focus on the well studied case of parallel flow over a porous layer. Furthermore, we regard mass transport from the fluid region to the porous layer. As an application, we investigate a hypothetical electrochemical channel flow cell which includes a porous diffusion layer covering the anode. Such a structure is close to a fuel cell electrode which usually includes a porous diffusion layer, and therefore the investigation of the influence of the interface between free and porous media flow on solute transport processes appears to be of considerable interest. For the proposed structure, we can use Poiseuille like solutions to obtain coupled free and porous media flow velocity fields. In particular, we model the *limiting current behavior* of such a cell with special emphasis on the impact of the fluid-porous interface.

The difficulty in finding effective coupling conditions at the interface between the channel flow and the porous layer lies in the fact that, when using stationary (Navier–)Stokes and Darcy’s equations to model flow in the two regions, the structures of the corresponding differential operators are different. Alternatively, when

---

2000 *Mathematics Subject Classification.* Primary: 65N99; Secondary: 35K20.

*Key words and phrases.* limiting current, finite volume method, fluid-porous interface problem.

The first and the third author are supported by the PAKT-Research Network *Coupled Fluid Flow in Energy and Environmental Research* of the Leibniz Association.

using the Brinkman model for the porous media, this difficulty does not occur: continuity of velocity and stress at the interface can be satisfied. But the validity of the Brinkman model for general porous media is discussed controversially, see [17].

We focus on three models: first on the coupling of the free flow with a Darcy medium, secondly the coupling with a Brinkman porous medium and finally we consider a three-layer configuration, where the porous medium is modeled by a Brinkman porous transition layer overlying a Darcy porous material. Exact analytical solutions can be devised from appropriate interface conditions [5, 11].

The evolution of the species concentration transported with the coupled free and porous media flow is modeled by a standard advection diffusion ansatz. Also, in simple geometries, analytical solutions do not exist, and for a significant range of flow rates of interest, asymptotic theory is not applicable even in the case without a porous layer, calling for numerical methods to obtain approximate solutions for the species concentration. The discretization method of our choice is the *finite volume method*. Due to upwinding, it is unconditionally stable also for high flow rates and thus is able to reproduce physical properties of the processes such as the positivity value of the concentration and the local maximum principle.

**2. Flow modeling.** The spatial domain  $\Omega$  under consideration with coordinate functions  $(x, y)$  is described as:  $\bar{\Omega} = \bar{\Omega}_p \cup \bar{\Omega}_f$ , where  $\Omega_f = (0, L) \times (0, H_f)$  is the free flow domain, and  $\Omega_p = (0, L) \times (-H_p, 0)$  denotes the porous part, cf. Fig. 1.

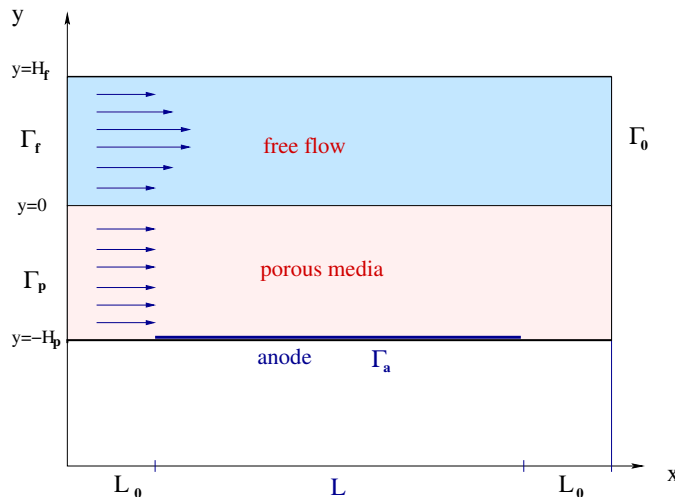


FIGURE 1. Schematic of a flow cell with porous diffusion layer

We characterize the porous medium with respect to the fluid flow by its permeability  $K = K(\varepsilon)$ , and with respect to species transport by its dispersion coefficient  $D_p$ . In order to simplify the discussion we relate both to the porosity  $\varepsilon$  of the porous medium. More precisely, we use the *Karman-Kozeny equation* [1]

$$K = K_0 \frac{\varepsilon^3}{(1 - \varepsilon)^2} \quad (1)$$

and the *Bruggeman correlation*  $D_p = D_f \varepsilon^{\frac{3}{2}}$ , cf. [18].

We consider a steady-state flow process in a free flow domain modeled by the *incompressible Navier-Stokes equation*

$$-\mu\Delta\vec{v} + (\rho\vec{v} \cdot \nabla)\vec{v} = -\nabla p, \quad \nabla \cdot \vec{v} = 0, \quad (x, y) \in \Omega_f. \quad (2)$$

Every channel flow profile satisfies the *no-slip condition* at the impermeable wall

$$v(y) = 0 \quad \text{at } y = H_f, \quad (3)$$

and due to the incompressibility condition  $\nabla \cdot \vec{v} = 0$  one immediately obtains the continuity of the normal velocity across the fluid-porous interface at  $y = 0$ .

We assume several flow profiles in the joint domain which are motivated by different approaches to model and to couple the problems in the free and porous flow regions. For all flow profiles, let  $1/\mu\nabla p = (\delta_p, 0)^\top$  be the constant pressure gradient with  $\delta_p < 0$ .

**2.1. Stokes-Darcy.** Here we consider a Stokes flow in the channel and a Darcy flow in the porous medium

$$\mu K^{-1}v = -p_x, \quad \nabla \cdot v = 0 \quad \text{in } \Omega_p, \quad (4)$$

with  $\mu$  the fluid dynamic viscosity,  $K$  is the permeability. Generally,  $v$  denotes the volumetric average of the velocity and  $p$  is the average of the pressure.

Since the two partial differential equations (2) and (4) have different structure, the *Beavers-Joseph coupling condition* [3] for tangential flow was proposed

$$\frac{dv}{dy}(0+) = \frac{\alpha}{\sqrt{K}} (v(0+) - v^D), \quad y = 0, \quad (5)$$

where  $v^D = -K\delta_p$  denotes the mean filtration velocity (Darcy velocity) and  $\alpha$  is the *Beavers-Joseph constant*. It denotes a dimensionless quantity depending on the material parameters which characterize the structure of the permeable material within the boundary region. The interface condition (5) replaces the classical condition of vanishing tangential velocity and allows for a discontinuity in the tangential velocity, taking into account rapid changes in the velocity in a small boundary layer by introducing a velocity jump.

We note that in the original paper by Beavers and Joseph [3], the coupling condition (5) has been derived in order to interpret an experiment with parallel channel flow in a porous medium and free space, very much similar to the structure proposed here. In their experiment, the amounts of fluid leaving the device at the porous part and at the free flow part have been separated, and measured for different values of the pressure drop. For this setting the exact analytical solution is easily obtained [5], and can be used in transport computations.

**2.2. Stokes-Brinkman.** Neale and Nader [16] suggested in 1974 the usage of the Brinkman correction [4] to the Darcy model:

$$-\nabla \cdot (\mu_{\text{eff}} \nabla \vec{v}) + \mu K^{-1} \vec{v} = -\nabla p, \quad \nabla \cdot \vec{v} = 0 \quad \text{in } \Omega_p, \quad (6)$$

where  $\mu_{\text{eff}} = \mu/\varepsilon$  is the *effective viscosity* of the fluid in  $\Omega_p$ . This model is usually used to account for the *high porosity* or to impose no-slip conditions on solid walls.

This flow profile is motivated by the coupling between Stokes and Brinkman equations which is convenient as it involves equations of similar type, and the coupling condition at the fluid-porous interface can be described by continuity of pressure, velocity and stress (using  $\mu_{\text{eff}}$ ). For this reason, it has been used in several complex simulation ansatzes, e.g. [12]. Moreover, Neal and Nader obtained in the fluid

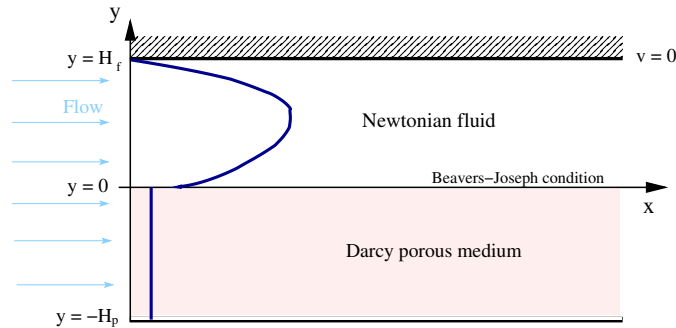


FIGURE 2. Two-layer configuration for Poiseuille flow overlying a porous medium (Darcy): velocity is significantly discontinuous at interface

region the same solution as Beavers and Joseph provided that the slip coefficient is chosen as  $\alpha = \sqrt{\mu_{\text{eff}}/\mu}$ . An exact analytical solution for a velocity profile in  $x$  direction can be found in [10].

Recently, Le Bars and Worster [14] considered special 'analytically tractable' cases for the one-domain approach with the Brinkman model for the porous medium. The authors compared their findings with the Stokes-Darcy approach of the preceding subsection 2.1 using the Beavers-Joseph condition (5). Le Bars and Worster considered the Brinkman equation in the original configuration studied by Beavers and Joseph, and found a new condition at the fluid-porous interface

$$v(-\delta+) = v^D(-\delta), \quad \text{with } \delta = c\sqrt{K}, \quad (7)$$

where  $c$  is a constant of order 1. They defined a *viscous transition zone* inside  $\Omega_p$ , where the Stokes equation still applies up to a depth  $\delta$ , and imposed continuity of pressure and velocities at the position  $y = -\delta$  (cf. Fig. 3). Here,  $\delta$  denotes the characteristic size of this transition zone (a few pore lengths). Using this new condition (7) the computed values have a (slightly) better coincidence with the experimental values of Beavers and Joseph.

**2.3. Stokes-Brinkman-Darcy.** There are serious doubts about the validity of the Brinkman equation, e.g. for the case of lower porosities [17, 11], whereas Darcy's law is not disputed for this case. The Brinkman model suffers from at least three limitations: first it is only valid for materials with high porosity, secondly, the effective viscosity  $\mu_{\text{eff}}$  used in this model may change discontinuously at the interface. Finally, as a rule of thumb, the Brinkman model should only be used if the Reynolds numbers  $\text{Re} = \rho UL/\mu$  of the corresponding free flow is greater than 10. Here  $U$  and  $L$  are characteristic values for the velocity and the length of the whole problem.

On the other hand, it appears to be useful to introduce a transition layer between Stokes and Darcy flow, which may be described by the Brinkman equation. For this setting, the exact analytical solution for the velocity profile is given in [11].

**3. Species transport modeling.** At fixed temperature  $T$  and fixed pressure  $p$ , a  $\text{H}_2\text{SO}_4$  based electrolyte containing dissolved  $\text{H}_2$  enters the cell at the inlet, flows over the anode, and leaves the cell at an outlet. At the inlet, the solute concentration is given by a value  $c_I$ , which depends on the pressure and the temperature.  $\text{H}_2$  is

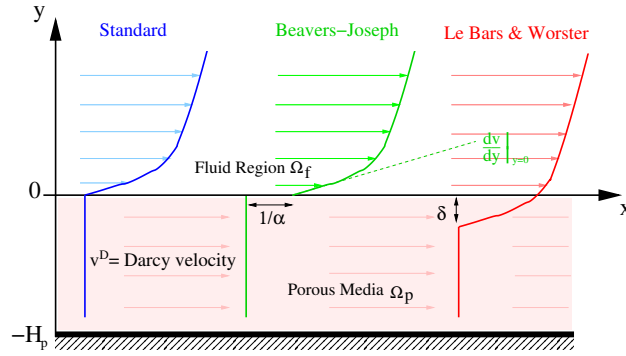


FIGURE 3. Comparison of Different Interface Models for Porous Media: From left to right: The standard case: no-slip condition on the fluid–porous interface, the Beavers–Joseph condition (5): slip of size  $1/\alpha$  on the fluid–porous interface and the Le Bars and Worster condition (7): slip by  $\delta$  into the porous media.

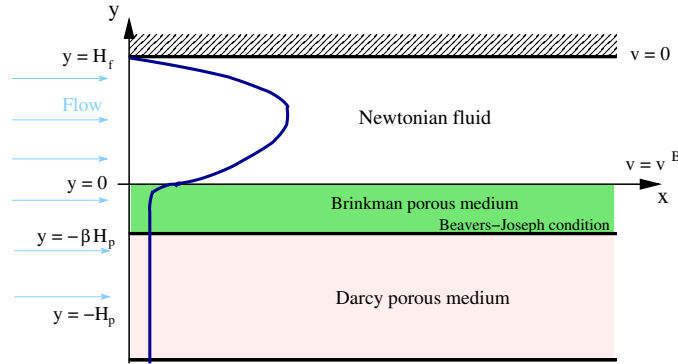


FIGURE 4. Three–layer configuration for Poiseuille flow overlying a porous medium with Brinkman transition layer: still discontinuity in velocity between Brinkman and Darcy layers with relative error  $\gamma \sim 1/\beta$  of lower order

transported to the anode and reacts at the catalytic surface according to



creating two electrons and two protons per reacted molecule. The amount of electrons generated during this reaction is measured as an electrical current. For high enough ion concentration due to the support electrolyte, ohmic potential drops are negligible. Furthermore, the reaction rate of hydrogen oxidation is large in comparison to the transport processes in the cell, therefore we say that it is *purely transport limited*. The current  $I$  measured in such a situation is called *limiting current*.

**3.1. Transport equation.** According to [8, 9] the stationary species transport (convection and diffusion) in such a flow cell can be described by the partial differential equation

$$\nabla \cdot (D(x, y) \nabla c - c \vec{v}(x, y)) = 0 \quad \text{in } \Omega \quad (9)$$

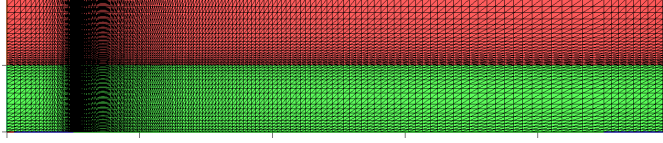


FIGURE 5. Aligned computational grid.

supplied with the incompressibility condition  $\nabla \cdot \vec{v} = 0$ . Here,  $D$  is the molecular diffusion coefficient and  $c = c(x, y)$  denotes the concentration of a dissolved species.

Let us assume that the diffusion coefficient  $D = D(x, y)$  is piecewise constant:  $D(x, y) = D_f$  for  $y > 0$  and  $D(x, y) = D_p$  for  $y < 0$  and for the velocity profile, we assume  $\vec{v}(x, y) = (v_x(y), 0)^\top$  with a given  $x$  component  $v_x(y)$ , which has been discussed in the previous section. In the sequel, we will write shortly  $v(y)$  instead of  $v_x(y)$ . We consider the following boundary conditions:

$$c = c_f \quad \text{on } \Gamma_f = 0 \times (0, H_f) \quad (\text{free flow inlet}) \quad (10a)$$

$$c = c_p \quad \text{on } \Gamma_p = 0 \times (-H_p, 0) \quad (\text{porous inlet}) \quad (10b)$$

$$c = 0 \quad \text{on } \Gamma_a = (L_o, L - L_o) \times -H_p \quad (\text{anode}) \quad (10c)$$

$$\frac{\partial c}{\partial \vec{n}} = 0 \quad \text{on } \Gamma_o = L \times (-H_p, H_f) \quad (\text{outlet}) \quad (10d)$$

On all other parts of the domain, we assume *no flow boundary conditions*

$$(D(x, y)\nabla c - c\vec{v}(x, y)) \cdot \vec{n} = 0. \quad (11)$$

The values  $c_f$ ,  $c_p$  in (10) denote the inlet concentrations. The boundary concentration at the anode will be assumed to be 0, modeling a surface reaction with infinitely fast kinetics. For reaction (8), the limiting current can be calculated from the amount of solute leaving the domain at the anode as

$$I = 2F \int_{\Gamma_a} (D(x, y)\nabla c - c\vec{v}(x, y)) \cdot \vec{n} ds. \quad (12)$$

**3.2. Asymptotic models.** Due to the lack of analytical solutions, asymptotic models based on boundary layer theory have been used for a long time to derive quantitative estimates. For the channel flow with an infinite strip electrode, the solution was given in [15]. In [8] the following expression for the limiting current was established

$$I = 2FD(c_I - c_0) \frac{A}{L} \text{Sh}, \quad (13)$$

where  $F$  the Faraday constant and

$$\text{Sh} = \frac{3^{\frac{4}{3}}}{2\Gamma(\frac{1}{3})} \text{Pe}^{\frac{1}{3}} \approx 0.8075491 \text{Pe}^{\frac{1}{3}}, \quad (14)$$

is the dimensionless Sherwood number,  $D$  the diffusion coefficient and  $A$  is the electrode surface, which in this case is equal to  $L$ . The dimensionless Peclet number  $\text{Pe}$  is defined by  $\text{Pe} = 6\bar{v}L^2/(DH_f)$ .

**4. Numerical experiments.** For discretizing (9), we use the Voronoi box based finite volume method [2] on aligned grids (cf. Figure 5) which has been shown to be able to reflect high flow rate asymptotics well [8]. The coupled model allows to discuss the influence of the coupling method on the possible measurement data.

4.1. **Thick porous layer.** Let  $L = 10$ ,  $L_o = 1$ ,  $H_p = 1$ ,  $H_f = 1$ , i.e. we assume that the porous layer and the free flow domain are of equal thickness.

**Undivided input.** First, we consider the case where  $c_f = c_p = 1$ , i.e. there is no divide at the inlet. For the Stokes-Brinkman ansatz, Figures 6, 7 essentially reveal

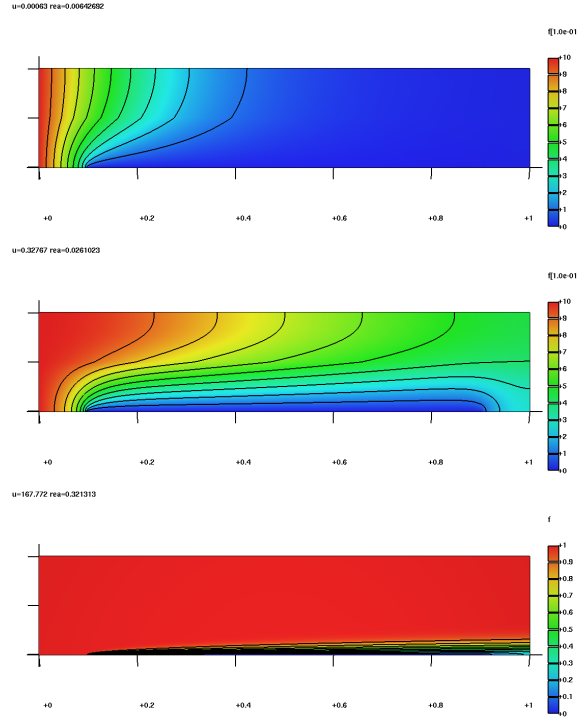


FIGURE 6. Stokes-Brinkman ansatz. Concentration regimes for thick porous layer and undivided inlet for porosity  $\epsilon = 0.6$ : low (top), medium (middle) and high (bottom) pressure gradients.

three regimes. The first, low pressure gradient regime is diffusion dominant, with small limiting current over several magnitudes of the pressure gradient. For medium pressure gradients, solute is transported through the cell, with moderate velocity, so that a pressure gradient to the anode can build up, however without creating a true boundary layer. At high pressure gradients, the porous media and free flow problems essentially decouple, and the limiting current is solely determined by the porous media flow. We observe a boundary layer, and an asymptotic behaviour. We note that the slope is higher than that of the classical Leveque solution (13).

**Divided input.** For divided input, i.e.  $c_f = 1$ ,  $c_p = 0$  we observe similar regimes, see the Figures 9, 10. However, it is clear, that the division in the high pressure gradient asymptotic leads to zero limiting current. From Figures 8 and 11 we establish that the dependence of the limiting current on the choice between Stokes-Brinkman and Stokes-Darcy resp. on the choice of  $\alpha$  is small, within the range of typical measurement errors. However, there is a large difference to the Darcy-Darcy case. At the other hand, the dependence on porous media data parameterized by  $\epsilon$  is significant.

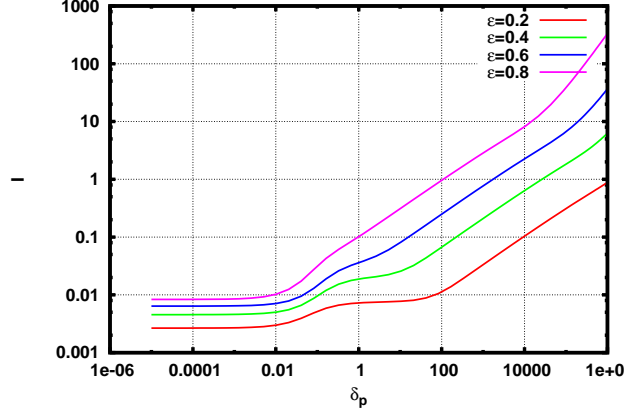


FIGURE 7. Limiting current  $I$  vs. pressure gradient  $\delta_p$  for different porosity values  $\epsilon$ .

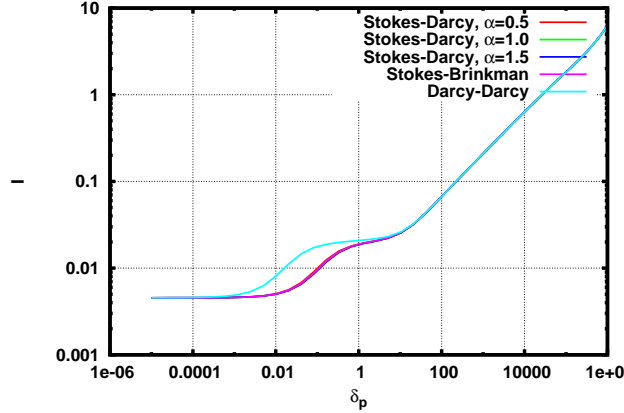


FIGURE 8. Thick porous layer, undivided input. Limiting current  $I$  vs. pressure gradient  $\delta_p$  for  $\epsilon = 0.4$ . Comparison of Stokes-Brinkman, Stokes-Darcy and Darcy-Darcy with different values of slip coefficient  $\alpha$ .

**4.2. Thin porous layer.** Now we consider a thin porous layer of thickness  $H_p = 0.1$  and get a different picture. As in this case, the Darcy and Brinkman velocities close to the electrode differ substantially, the boundary layer there is strongly influenced by this choice, so there is a significant difference between the Stokes-Brinkman and the Stokes-Darcy model, in the same order of magnitude as the difference to the Darcy-Darcy case. On the other hand, as an important outcome, we observe an insignificant dependence on the Beavers-Joseph slip coefficient  $\alpha$ .

**Undivided input.** In Figures 12-13 we consider the undivided input case  $c_f = c_p = 1$ . For this case we observe in Figure 12 the expected behaviour: the limiting current increases with increasing porosity  $\epsilon$ . Figure 13 shows only a weak dependence of the limiting current from the chosen fluid-porous model; only a small deviation is visible.

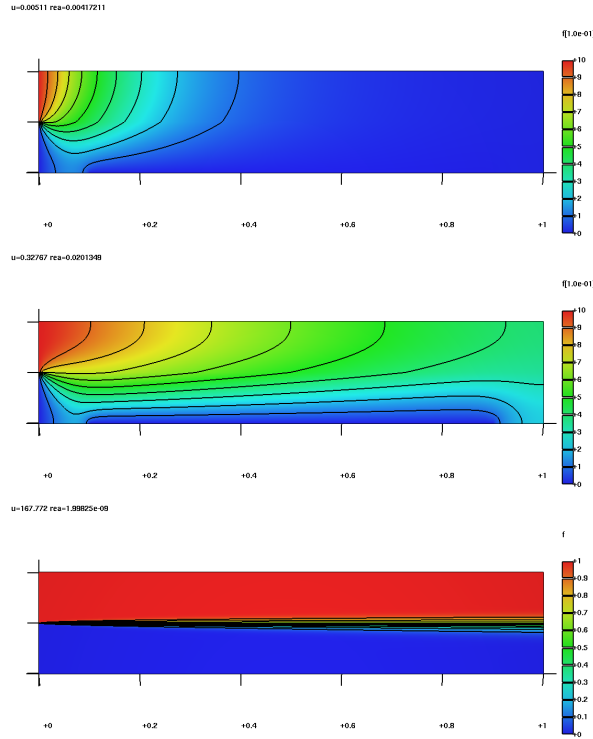


FIGURE 9. Thick porous layer, divided input, Stokes-Brinkman ansatz. Concentration regimes for thick porous layer and divided inlet concentration for  $\epsilon = 0.6$ : low (top), medium (middle) and high (bottom) pressure gradients.

**Divided input.** Now, in the following Figures 14-15 we present the results of the corresponding divided input case  $c_f = 1$ ,  $c_p = 0$  for a thin porous layer. Figure 14 shows the expected behaviour: for most values of pressure gradient  $\delta_p$  the limiting current increases with increasing porosity  $\epsilon$ . The division in the high pressure gradient asymptotic leads to zero limiting current. Figure 15 shows only a weak dependence of the limiting current from the chosen value for the slip coefficient  $\alpha$ . But the selection of the fluid-porous model leads to strong deviations.

5. **Outlook.** The discussed numerical model allows to investigate experimental setups which combine free flow and porous flow regions, similar to those in fuel cells, especially in microfluidic fuel cells [13]. In order to describe these more complex devices, the model needs can be extended by multiple transported and reacting species, similar to [6]. Of considerable interest is the numerical solution of the coupled free and porous media flow in geometrical cases more general in comparison to those described here. A finite volume method for this case is currently under development.

## REFERENCES

- [1] G. Arampatzis and D. Assimacopoulos, *Numerical modeling of convection-diffusion phase change problems*, *Comput. Mech.*, **21** (1998), 409–415.

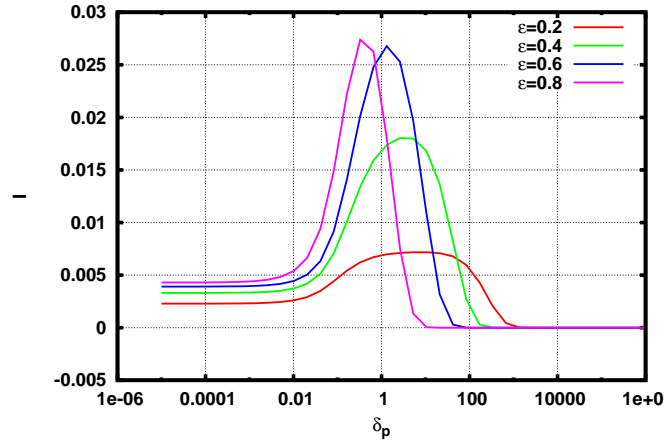


FIGURE 10. Thick porous layer, divided input, Stokes-Brinkman ansatz.  $I$  vs.  $\delta_p$  for different porosity values  $\varepsilon$ .

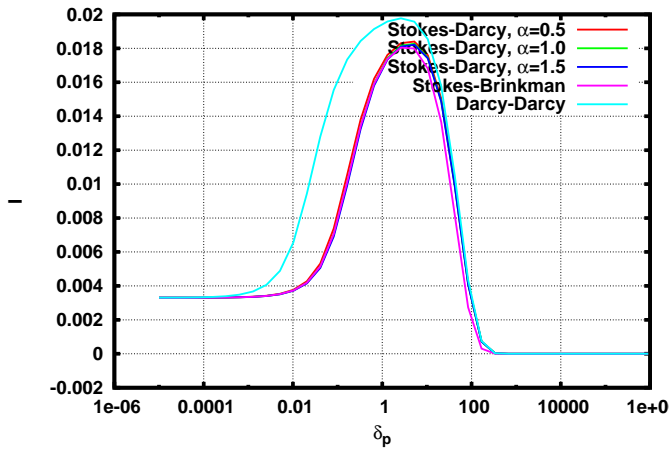


FIGURE 11. Thick porous layer, divided input.  $I$  vs.  $\delta_p$  for porosity  $\varepsilon = 0.4$ . Comparison of Stokes-Brinkman, Stokes Darcy and Darcy-Darcy with different values of slip coefficient  $\alpha$ .

- [2] R.E. Bank and D.J. Rose, *Some error estimates for the box method*, SIAM J. Numer. Anal., **24** (1987), 777–787.
- [3] G.S. Beavers and D.D. Joseph, *Boundary conditions at a naturally permeable wall*, J. Fluid Mech., **30** (1967), 197–207.
- [4] H.C. Brinkman, *A calculation of the viscous force exerted by a flowing fluid on a dense swarm of particles*, Appl. Sci. Res. A, **1** (1948), 27–34.
- [5] M.H. Chang, F. Chen and B. Straughan, *Instability of Poiseuille flow in a fluid overlying a porous layer*, J. Fluid Mech., **564** (2006), 287–303.
- [6] J. Divisek, J. Fuhrmann, K. Gärtner and R. Jung, *Performance Modeling of a Direct Methanol Fuel Cell*, J. Electrochem. Soc., **150** (2003) 6, A811–A825.
- [7] M. Ehrhardt, J. Fuhrmann, E. Holzbecher and A. Linke, *Mathematical Modeling of Channel-Porous Layer Interfaces in PEM Fuel Cells*, in: B. Davat and D. Hissel (ed.), Proceedings of ‘FDFC2008 – Fundamentals and Developments of Fuel Cell Conference 2008’, Nancy, France.

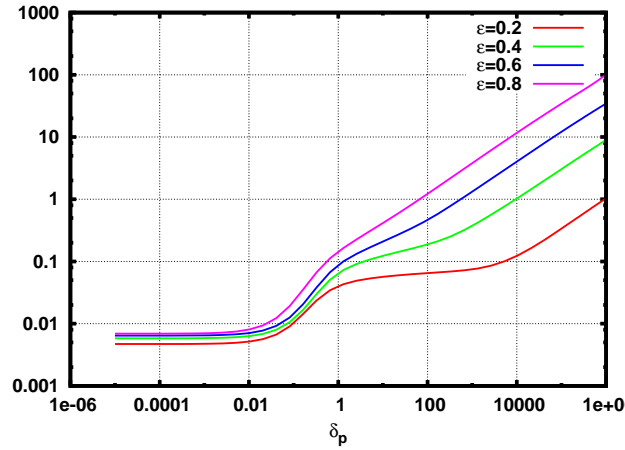


FIGURE 12. Thin porous layer, undivided input, Stokes-Brinkman ansatz.  $I$  vs.  $\delta_p$  for different porosity values  $\epsilon = 0.2, 0.4, 0.6, 0.8$ .

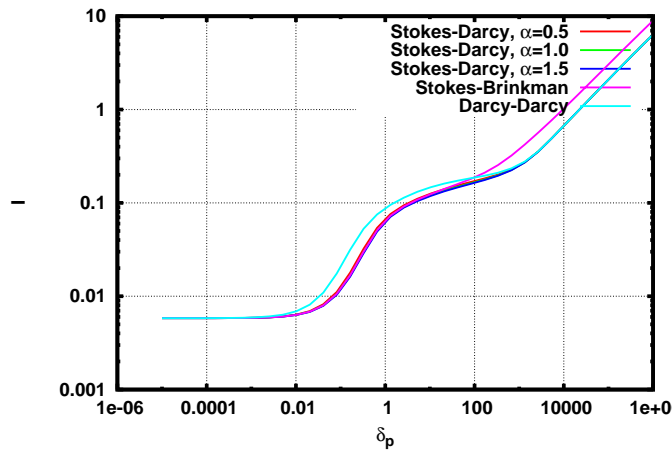


FIGURE 13. Thin porous layer, undivided input.  $I$  vs.  $\delta_p$  for porosity  $\epsilon = 0.4$ . Comparison of Stokes-Brinkman, Stokes-Darcy and Darcy-Darcy with different values of slip coefficient  $\alpha$ .

- [8] J. Fuhrmann, H. Zhao, E. Holzbecher, H. Langmach, M. Chojak, R. Halseid, Z. Jusys and R. Behm, *Experimental and numerical model study of the limiting current in a channel flow cell with a circular electrode*, Phys. Chem. Chem. Phys., **10** (2008), 3784–3795.
- [9] J. Fuhrmann, H. Zhao, E. Holzbecher and H. Langmach *Flow, transport, and reactions in a thin layer flow cell*, J. Fuel Cell Sci. Techn., **5** (2008), 021008/1–021008/10.
- [10] B. Goyeau, D. Lhuillier, D. Gobin and M.G. Velarde, *Momentum transport at a fluid-porous interface*, Int. J. Heat Mass Transfer, **46** (2003), 4071–4081.
- [11] A.A. Hill and B. Straughan, *Poiseuille flow in a fluid overlying a porous medium*, J. Fluid Mech., **603** (2008), 137–149.
- [12] O. Iliev and V. Laptev, *On numerical simulation of flow through oil filters*, Comput. Visual. Sci., **6** (2004), 139–146.
- [13] E. Kjeang, N. Djilali and D. Sinton *Microfluidic fuel cells: A review* J. Power Sources, 186 (2009) 353–369.

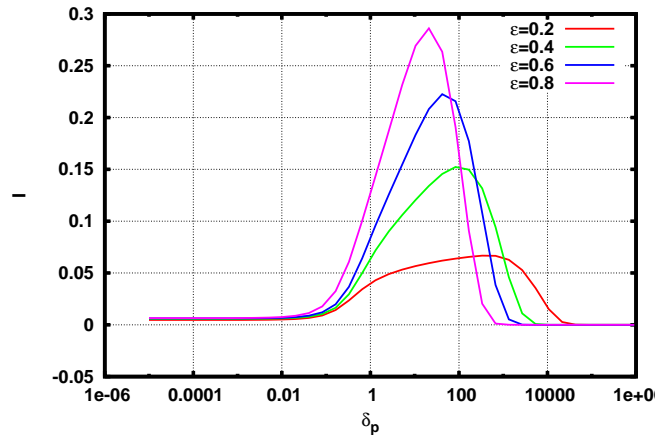


FIGURE 14. Thin porous layer, divided input, Stokes-Brinkman ansatz.  $I$  vs.  $\delta_p$  for different porosity values  $\epsilon = 0.2, 0.4, 0.6, 0.8$ .

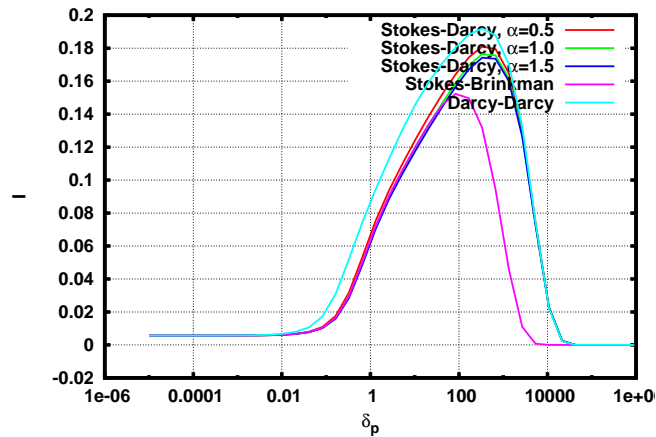


FIGURE 15. Thin porous layer, divided input.  $I$  vs.  $\delta_p$  for  $\epsilon = 0.4$ . Comparison of Stokes-Brinkman, Stokes-Darcy and Darcy-Darcy with different values of slip coefficient  $\alpha$ .

- [14] M. Le Bars and M.G. Worster, *Interfacial conditions between a pure fluid and a porous medium: implications for binary alloy solidification*, J. Fluid Mech. **550** (2006), 149–173.
- [15] A. L ev eque, *Annales des Mines*, **13** (1928), 201–299, 305–362, 381–415.
- [16] G. Neale and W. Nader, *Practical significance of Brinkman extension of Darcy’s law: coupled parallel flows within a channel and a bounding porous medium*, Can. J. Chem. Eng., **52** (1974), 475–478.
- [17] D.A. Nield, *The boundary correction for the Rayleigh-Darcy problem: limitations of the Brinkman equation*, J. Fluid Mech., **128** (1983) 37–46.
- [18] J.G. Pharoah, K. Karan and W. Sun, *On effective transport coefficients in PEM fuel cell electrodes: Anisotropy of the porous transport layers*, J. Power Sources **161** (2006), 214–224.

Received October 2009

*E-mail address*: ehrhardt@math.uni-wuppertal.de, {fuhrmann|linke}@wias-berlin.de